NeuroImage: Clinical 9 (2015) 498–505

Contents lists available at ScienceDirect

NeuroImage: Clinical

journal homepage: www.elsevier.com/locate/ynicl

Structural connectivity of the anterior cingulate in children with unilateral cerebral palsy due to white matter lesions

Simon M. Scheck[a,b], Kerstin Pannek[a,b,c], David A. Raffelt[d], Simona Fiori[e], Roslyn N. Boyd[b], Stephen E. Rose[c,*]

[a] School of Medicine, University of Queensland, Brisbane, Australia
[b] Queensland Cerebral Palsy and Rehabilitation Research Centre, University of Queensland, Brisbane, Australia
[c] Australian e-Health Research Centre, CSIRO, Brisbane, Australia
[d] Florey Institute of Neuroscience and Mental Health, Melbourne, Victoria, Australia
[e] Department of Developmental Neuroscience, Stella Maris Scientific Institute, Pisa, Italy

ARTICLE INFO

Article history:
Received 2 August 2015
Received in revised form 8 September 2015
Accepted 22 September 2015
Available online 30 September 2015

ABSTRACT

In this work we investigate the structural connectivity of the anterior cingulate cortex (ACC) and its link with impaired executive function in children with unilateral cerebral palsy (UCP) due to periventricular white matter lesions.

Fifty two children with UCP and 17 children with typical development participated in the study, and underwent diffusion and structural MRI. Five brain regions were identified for their high connectivity with the ACC using diffusion MRI fibre tractography: the superior frontal gyrus, medial orbitofrontal cortex, rostral middle frontal gyrus, precuneus and isthmus cingulate. Structural connectivity was assessed in pathways connecting these regions to the ACC using three diffusion MRI derived measures: fractional anisotropy (FA), mean diffusivity (MD) and apparent fibre density (AFD), and compared between participant groups. Furthermore we investigated correlations of these measures with executive function as assessed by the Flanker task.

The ACC–precuneus tract had significantly different MD ($p < 0.0001$) and AFD ($p = 0.0072$) between groups, with post-hoc analysis showing significantly increased MD in the right hemisphere of children with left hemiparesis compared with controls. The ACC–superior frontal gyrus tract had significantly different FA ($p = 0.0049$) and MD ($p = 0.0031$) between groups. AFD in this tract (contralateral to side of hemiparesis; right hemisphere in controls) showed a significant relationship with Flanker task performance ($p = 0.0045$, $\beta = -0.5856$), suggesting that reduced connectivity correlates with executive dysfunction.

Reduced structural integrity of ACC tracts appears to be important in UCP, in particular the connection to the superior frontal gyrus. Although damage to this area is heterogeneous it may be important in early identification of children with impaired executive function.

1. Introduction

Cerebral palsy (CP) is a non-progressive disability caused by a heterogeneous group of brain pathologies. The clinical phenotype has been classically described in terms of motor impairment (Krägeloh-Mann and Cans, 2009), and consequently there has been a large focus in neurological research around motor regions of the brain in these children (Krägeloh-Mann and Cans, 2009; Arnfield et al., 2013; Krägeloh-Mann and Horber, 2007; Scheck et al., 2012). There has been increasing interest in exploring cognitive and social functioning in children with CP (Whittingham et al., 2014; Bodimeade et al., 2013; Weierink et al., 2013; Bjorgaas et al., 2012; Caillies et al., 2012; Hustad et al., 2012; Iwata et al., 2012), showing impairments across multiple executive function domains (Bodimeade et al., 2013) with considerable impact on everyday life (Whittingham et al., 2014). Up to 50% of children with CP have an intellectual disability (Novak et al., 2012) and 25–50% have attention deficit disorder or attention deficit hyperactivity disorder (Bjorgaas et al., 2012; Novak et al., 2012). Despite extensive research on the impact of cognitive and social impairment on the lives of people with CP, there is little understanding of the underlying neuropathology (Weierink et al., 2013).

Abbreviations: ACC, anterior cingulate cortex; AFD, apparent fibre density; CP, cerebral palsy; CTD, children with typical development; DTI, diffusion tensor imaging; FA, fractional anisotropy; FOD, fibre orientation distribution; HARDI, high angular resolution diffusion imaging; MD, mean diffusivity; MRI, magnetic resonance imaging; ROI, region of interest; SIFT, spherical deconvolution informed filtering of tractograms; UCP, unilateral cerebral palsy; WM, white matter.

* Corresponding author at: Australian e-Health Research Centre, Level 5, UQ Health Sciences Building, Royal Brisbane and Women's Hospital, Herston, QLD 4029, Australia. Tel.: +617 32533620, fax: +617 32533690.
E-mail address: Stephen.Rose@csiro.au (S.E. Rose).

http://dx.doi.org/10.1016/j.nicl.2015.09.014

Lesions in CP typically involve periventricular white matter (56%) or either cortical or deep grey matter (18%), with global maldevelopments being less common (9%) (the remaining 17% are non-specific) (Krägeloh-Mann and Horber, 2007). In the present study we assess children with periventricular white matter (WM) lesions. Early WM damage evident on structural MRI at term equivalent age is a significant predictor of executive function in very preterm children (Iwata et al., 2012), and diffusion properties of multiple WM regions have been shown to correlate with neuropsychological scores in children with spastic diplegia (Rai et al., 2013). In a whole brain connectome study in children with unilateral CP with WM lesions we have shown that the integrity of tracts connecting to the anterior cingulate cortex (ACC) may be compromised (Pannek et al., 2014).

The ACC is a bilateral cortical structure in the medial wall of the brain, important for both cognitive and social functioning (Bush et al., 2000). Functional MRI studies have shown that the ACC plays a central role within the executive function brain network (Botvinick et al., 1999), being highly connected with the prefrontal cortex, premotor and supplementary motor areas and parietal cortex (Paus, 2001; Devinsky et al., 1995).

To investigate WM integrity, we used two models derived from diffusion weighted MRI: the diffusion tensor model; and constrained spherical deconvolution. Multiple MRI measurements of Brownian motion of water molecules (Stejskal, 1965) are acquired for each voxel, used to derive a mathematical model from which various properties can be extracted, relating to underlying tissue. The majority of diffusion MRI studies in children with CP to date have utilised the diffusion tensor model (see review Scheck et al., 2012) which characterises diffusion within each voxel using a single tensor ellipsoid (Basser et al., 1994). From the tensor, quantitative measures such as fractional anisotropy (FA; often reported as a surrogate marker for white matter 'integrity') and mean diffusivity (MD) can be computed (Basser and Pierpaoli, 1996). Tractography algorithms can also exploit tensor-derived fibre orientation information to estimate fibre bundle trajectories (Mori et al., 1999). Surrogate markers for tract based 'connectivity' can then be computed by averaging quantitative measures within voxels traversed by tractography streamlines.

Where complex WM architecture exists, multiple fibres may cross within each voxel, and single ellipsoid tensor orientations can no longer be reliably used for tractography. FA results in these regions can be unintuitive and difficult to interpret (Douaud et al., 2011; Pierpaoli et al., 2001). A higher order model of the diffusion signal is therefore more appropriate (Jones, 2010). The fibre orientation distribution (FOD), computed via constrained spherical deconvolution, is one such model (Tournier et al., 2004, 2007). By resolving multiple fibres within each voxel, the FOD provides more accurate fibre directions for tractography in addition to tract specific quantification of white matter. The apparent fibre density (AFD), a recently developed fibre specific metric derived from the FOD lobe parallel to the direction of the streamline (Raffelt et al., 2012a; Raffelt et al., 2013) allows a result that reflects the individual tract being analysed, in contrast with the diffusion tensor model which provides a voxel-average FA or MD value. The AFD has been used to identify tracts with reduced fibre density in Motor Neurone Disease (Raffelt et al., 2012a), Alzheimer's disease (Raffelt et al., 2012b), epilepsy (Vaughan et al., 2013), infants born preterm (Tournier et al., 2013), adolescents born preterm (Raffelt et al., 2014a), grey matter heterotopia (Farquharson et al., 2014), and Dravet Syndrome (Raffelt et al., 2014b).

In this work we set out to analyse the connectivity of the ACC using both AFD and traditional tensor-derived measures (as this is the currently accepted approach in the majority of diffusion imaging studies in CP). We expect that due to anatomical location, WM tracts projecting from the ACC will pass through a high number of voxels with multiple fibre orientations and therefore AFD analysis will be more specific to the tracts being analysed than diffusion tensor-based analysis. We also aim to determine whether performance in an executive function task correlates with connectivity measures of these tracts.

2. Methods

2.1. Participants

A total of 71 children were identified through a population-based research database, recruited for one or more clinical studies requiring baseline MRI and clinical assessment (prior to any study specific intervention). Selection criteria included age 3–17 years, a confirmed diagnosis of unilateral cerebral palsy, attendance at a mainstream school, and a score of II (two) or below in both the Gross Motor Function Classification System (GMFCS) (Russell et al., 1989) and Manual Ability Classification System (MACS) (Eliasson et al., 2006) as assessed by an occupational therapist (scores shown in Table 1).

Of these children, 53 were selected based on MRI brain image classification. Images were reviewed by a child neurologist (SF) and classified according to the Krageloh-Mann classification system (Krägeloh-Mann and Horber, 2007) as periventricular white matter lesions (the remainder included 16 with cortical or deep grey matter lesions and 2 with brain malformations). Of these, 52 children were able to be adequately parcellated by the software as outlined below. These children were aged 5–17 years, and included 25 with left hemiparesis and 27 with right hemiparesis.

Seventeen children with typical development (CTD) without brain pathology were also included in all analyses as controls. The institutional review board approved the study and written informed consent was obtained from a parent or guardian, as well as verbal assent from each child.

2.2. Flanker task

A subset of children (7 left hemiparesis, 10 right hemiparesis, 14 CTD) participated in the Flanker task (Eriksen and Eriksen, 1974), which has previously been shown to be strongly linked to the ACC using functional MRI (Brown, 2009). This involved five symbols displayed in a horizontal line on a computer screen. The central symbol was either a left or right facing arrow. The remaining four symbols (the "Flanker" objects) were either congruent (e.g. ← ← ← ← ←); incongruent (e.g. → → ← → →); or neutral (e.g. – – ← – –). Subjects were given 5 s to press either the right or left button on a handheld control (using their preferred hand) to indicate the direction of the central arrow. This was repeated 120 times, with a 30 s break every after each set of 40 trials. To eliminate any group differences in motor performance, we used the mean time taken for a correct answer in the neutral condition as a baseline, and reported the mean additional time needed for a correct answer in the incongruent condition as a measure of executive function (increased additional time representing poorer executive function). Results were statistically corrected for age (and gender where significant) using a general linear model (see Statistical analysis below). We assessed the relationship between task performance and diffusion derived metrics (FA, MD and AFD) in both hemispheres, labelled as "contralateral" or "ipsilateral", referring to the side of hemiparesis. For CTD ipsilateral was arbitrarily taken as the left hemisphere (as this is ipsilateral to the non-dominant hand in right handers, but still the non-dominant hemisphere in most left handers (Knecht et al., 2000)).

Table 1
Participant information. Age given as mean ± standard error. CTD — children with typical development. GMFCS — Gross Motor Function Classification System. MACS — Manual Ability Classification Scale.

			Gender		GMFCS		MACS	
Group	n	Age	F	M	I	II	I	II
CTD	17	10.6 ± 0.5	10	7	n/a	n/a	n/a	n/a
Left hemiparesis	25	9.9 ± 0.6	10	15	20	5	15	10
Right hemiparesis	27	11.4 ± 0.6	10	17	18	9	11	16

2.3. Image acquisition

High resolution structural images were acquired for each participant using a 0.9 mm isotropic 3D T1-weighted magnetisation-prepared gradient-echo (MPRAGE) sequence using a 3 T MRI scanner (Siemens, Erlangen, Germany). The acquisition parameters were: FOV 24 × 25.6 × 17.6 cm, TR/TE/TI 2300/2.26/900 ms, flip and angle 9°. A high angular resolution diffusion imaging (HARDI) scan was performed using 60 axial slices, FOV 30 × 30 cm, TR/TE 9200/112 ms, 2.5 mm slice thickness, acquisition matrix 128 × 128 with a 2.3 mm in plane image resolution, an acceleration factor of 2 and a diffusion encoding gradient strength of b = 3000 s mm^{-2}. Sixty five diffusion weighted images were acquired at each location consisting of 1 low (b = 0) and 64 high diffusion weighted images. A field map was acquired using two 2D gradient recalled echo images (TE1/TE2 4.76/7.22 ms) to assist the correction for distortion due to susceptibility inhomogeneity.

2.4. Parcellation

Cortical reconstruction and volumetric segmentation were performed on T1 images with the Freesurfer image analysis suite (http://surfer.nmr.mgh.harvard.edu/). This involves removal of non-brain tissue followed by automated segmentation of cortical and subcortical structures (Fischl et al., 2002). Manual assessment was performed at each step and subjects were excluded if parcellation was either deemed to be inadequate or was unable to be processed. This resulted in exclusion of one subject (52 total included as well as 17 controls).

2.5. Diffusion preprocessing and tractography

Diffusion weighted images were corrected for subject motion by identifying volumes with head movement between subvolumes of the interleaved acquisition (i.e. within volumes) using the discontinuity index (Nam and Park, 2011) and subsequently using the FMAM (Fit Model to All Measurements) method to correct movement between volumes (Bai and Alexander, 2008). Susceptibility distortions were corrected using the field map employing FUGUE (Jenkinson, 2003) and PRELUDE (Jenkinson, 2004) in raw image space (both contained within FMRIB's Software Library (FSL) (Jenkinson et al., 2012)), with signal intensity correction (Jones and Cercignani, 2010). Motion artefacts were identified and replaced using Detection and Replacement of Outliers Prior to Resampling (DROP-R) (Morris et al., 2011), modified from the originally proposed method to incorporate an outlier detection technique suitable for high b-value diffusion data (Pannek et al., 2012). All images were normalised by dividing each diffusion weighted volume by the median value of all WM voxels in the b = 0 image. Using the corrected data, the fibre orientation distribution (FOD) was estimated using the constrained spherical deconvolution method within the MRtrix package (http://www.mrtrix.org) (Tournier et al., 2007). The response function used to derive the FOD was representative of the group, created by taking the mean response function from all children with typical development and an equal number of children with CP (selected using a random number generator). Fibre tracking was also performed using MRtrix. Bidirectional streamlines were seeded in the anterior cingulate (n = 100,000 each side), using a termination mask obtained from the structural image to ensure that streamlines remained within brain tissue (Pannek et al., 2010).

2.6. Connectivity analysis

The region of interest (ROI) used to drive the tractography analysis consisted of the Freesurfer parcellations of both caudal and rostral anterior cingulate (see Fig. 1 for example parcellation). The number of streamlines passing through every other cortical and subcortical ROI was calculated. ROIs appropriate for further connectivity analysis were selected based on the greatest number of ACC streamlines in the CTD group.

As our methodology is novel in this population, the corticospinal tract (CST) was also included as it has been well studied in this population using diffusion imaging (Scheck et al., 2012). The CST was derived using precentral gyrus, brainstem, thalamus and cerebellum parcellations. Bidirectional streamlines were seeded in the left and right precentral gyrus, again using the termination mask. Streamlines were selected if they reached the brainstem (a single parcellation, i.e. not divided into left and right) without passing through either the thalamus or cerebellum. Ten times more streamlines (i.e. n = 1,000,000) were required in this ROI to achieve similar streamline counts as the ACC tracts, due to the size of the ROI and spread of the seeded streamlines throughout the brain.

In this study we computed several measures as surrogate markers of tract connectivity. The first two measures were based on tensor-derived FA and MD. For each tract we computed the weighted mean of all FA and MD values across voxels traversed by tractography streamlines. A limitation of FA and MD is that they are voxel-average quantities, and are not tract-specific when unrelated tracts cross voxels traversed by the tract of interest. For this reason we also computed an alternative tract-specific connectivity measure based on AFD. At high diffusion gradient b-values (as used in this study) the AFD integral for a particular FOD 'lobe' is proportional to the intra-axonal volume of axons associated with that lobe (Raffelt et al., 2012a). By summing the AFD integral for all FOD lobes associated with the tract streamlines, a measure can be computed relating to the total intra-axonal tract volume (note that streamlines are associated with FOD lobes if the streamline tangent is within 30° of the FOD lobe peak orientation). However, since the total intra-axonal tract volume is a quantity that is tract length dependent, we divide by the mean streamline length to give a measure proportional to tract cross sectional area (something that should be more closely related to tract 'connectivity'). These calculations were performed using the 'afdconnectivity' command in MRtrix3 (http://www.mrtrix.org).

To assess the extent of crossing fibres within these tracts (and hence whether AFD would be more appropriate than FA and MD) a previously described technique was used (Jeurissen et al., 2013). This involved identifying the number of 'peaks' within each voxel, defined as FOD lobes with an amplitude greater than a threshold value (0.33). For each streamline the average number of peaks was calculated in each voxel traversed. We then assessed the percentage of voxels with more than one peak in each tract.

2.7. Statistical analysis

Statistical analysis was performed using StatSoft Statistica version 12. To determine difference between groups for tractography parameters we employed a general linear model incorporating age and gender. ANOVA was then used to assess whether there was a significant difference between groups (CTD, children with left hemiparesis and children with right hemiparesis) across the left and right hemispheres simultaneously. Where results were significantly different between groups, post-hoc analysis was performed using Dunnett's test (Dunnett, 1955) to determine in each hemisphere whether there was a significant difference between CTD and either children with left or right hemiparesis, correcting for multiple comparisons. Results were considered significant at $p < 0.05$.

A forward stepwise general linear model was employed to investigate the relationship between Flanker performance and diffusion metrics in all participants. Ipsilateral and contralateral hemispheres were investigated separately. A separate model was used for FA, MD and AFD. Age was included in the model, with extra variables (gender and tract metrics) being added to the model in a stepwise fashion until no remaining variables met statistical significance ($p < 0.05$). Where tracts were included into the model (i.e. met statistical significance) beta and p values were reported. This was all done in an automated fashion using StatSoft Statistica. To ensure that outliers were not giving false positive results Flanker scores were excluded if they fell more than two standard deviations outside the mean.

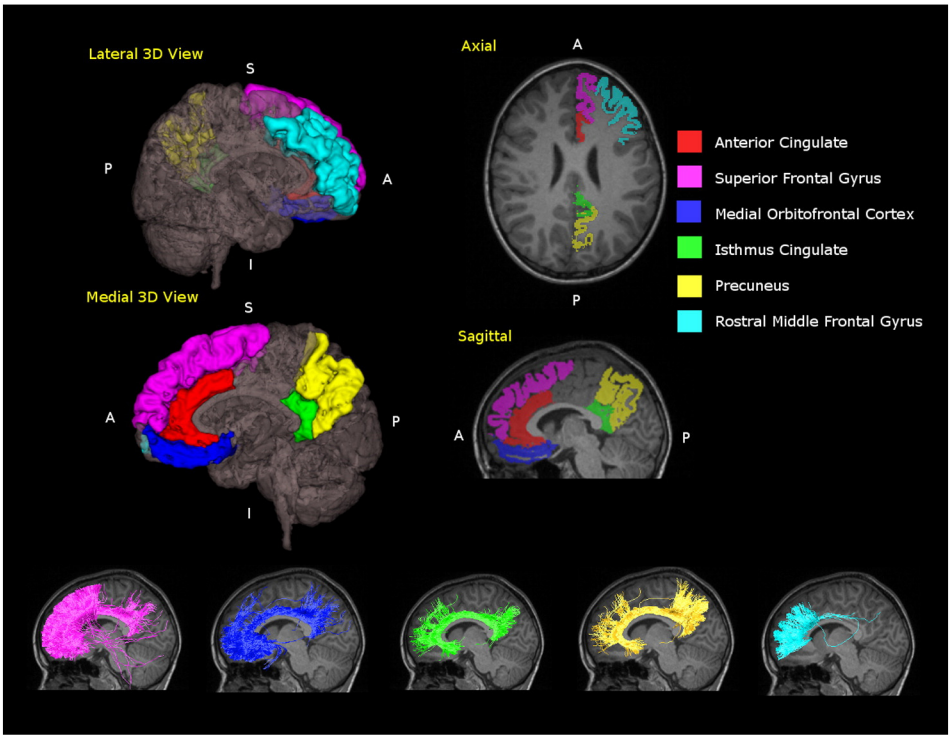

Fig. 1. Anatomical regions selected for highest streamline count (streamlines seeded in anterior cingulate cortex). Samples are from a child with typical development. Data is overlaid on T1 MRI (top right) and 3D reconstruction (top left) as well as tractograms projected on T1 MRI (bottom).

3. Results

3.1. Selection of tracts

The five regions reached by the largest number of streamlines generated in the ACC were, in order of highest to lowest, the superior frontal gyrus, medial orbitofrontal cortex, isthmus cingulate, precuneus and rostral middle frontal gyrus (examples shown in Fig. 1). This order was preserved in both hemispheres (intrahemispheric connections) for all groups. Streamline counts are shown in the Supplementary material.

3.2. Tract connectivity results

All FA, MD and AFD-based tract connectivity values with standard errors for selected tracts are shown graphically (corrected for

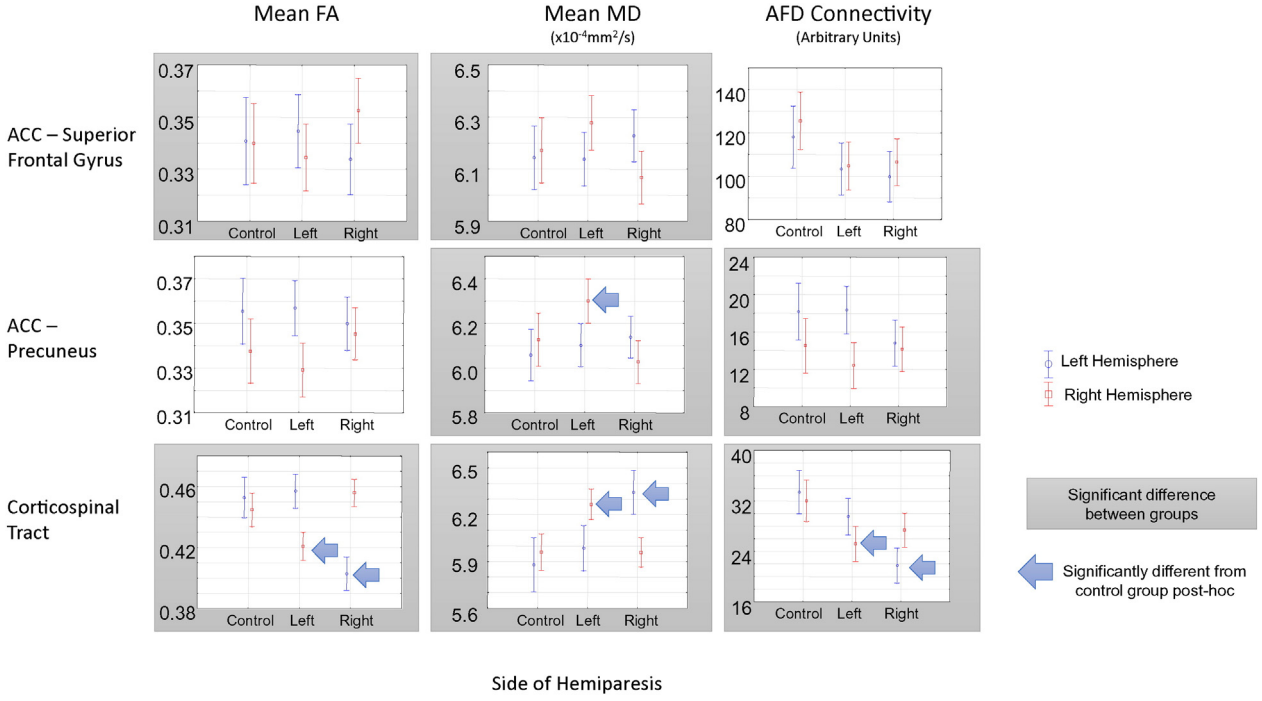

Fig. 2. Fractional anisotropy (FA), mean diffusivity (MD) and apparent fibre density (AFD) of tracts of interest in children with typical development (control) and children with left and right hemiparesis. Vertical bars denote 95% confidence intervals.

age and gender) in Fig. 2, with full raw data in the Supplementary material.

Streamlines connecting the ACC to the precuneus showed a significant difference in MD between groups ($p < 0.0001$). Post-hoc analysis showed significantly increased MD in the right hemisphere of children with left hemiparesis compared with CTD ($p = 0.0143$). AFD was also significantly different between groups ($p = 0.0072$), with no significant hemisphere specific differences between CTD and children with either left or right hemiparesis in post-hoc analysis.

Streamlines connecting the ACC to the superior frontal gyrus showed a significant difference between groups in both FA ($p = 0.0049$) and MD ($p = 0.0031$) but not AFD. In post-hoc analysis there were no significant hemisphere specific differences between CTD and children with either left or right hemiparesis.

Streamlines connecting the ACC to the isthmus cingulate (i.e. the cingulum bundle) showed a significant difference in MD between groups ($p = 0.0013$). Post-hoc analysis did not show any significant differences between CTD and children with either left or right hemiparesis. Neither FA nor AFD were significantly different between groups.

Streamlines connecting the ACC to the medial orbitofrontal cortex were not significantly different between groups for FA, MD or AFD. The same was true for streamlines connecting the ACC to the rostral middle frontal gyrus.

The CST showed a significant difference between groups in FA ($p < 0.0001$), MD ($p < 0.0001$) and AFD ($p < 0.0001$). Post-hoc analysis revealed that children with left hemiparesis had reduced FA ($p = 0.0005$), increased MD ($p < 0.0001$) and reduced AFD ($p = 0.0018$) compared with controls in the right hemisphere; and children with right hemiparesis had reduced FA ($p < 0.0001$), increased MD ($p = 0.0008$) and reduced AFD ($p < 0.0001$) compared with CTD in the left hemisphere.

3.3. Correlation with flanker scores

Children with hemiparesis took a significantly longer time (324 ± 80 ms; $n = 17$) to get a correct answer with the incongruent condition (compared with neutral condition) compared with CTD (110 ± 24 ms; $n = 14$) ($p = 0.0237$). Two scores were excluded from the correlation analysis as they were greater than two standard deviations beyond the mean. Both excluded scores belonged to children with left hemiparesis.

Assessing all participants, FA scores did not correlate with Flanker performance for any tracts. MD of the ipsilateral CST significantly correlated with Flanker performance ($p = 0.0412$, $\beta = 0.4020$). AFD of the streamlines connecting the ACC to the superior frontal gyrus in the contralateral hemisphere correlated with Flanker performance ($p = 0.0045$, $\beta = -0.5856$). These relationships are visualised in the supplementary data.

3.4. Crossing fibre analysis

More than 48% of voxels contained more than a single peak in all examined tracts. The CST had the highest percentage ($56.8\% \pm 1.0\%$), followed by the tracts connecting the ACC to the superior frontal gyrus ($53.8\% \pm 1.5\%$), medial orbitofrontal cortex ($53.3\% \pm 1.6\%$), precuneus ($52.0\% \pm 1.5\%$), rostral middle frontal gyrus ($50.0\% \pm 1.5\%$) and the isthmus cingulate cortex ($48.8\% \pm 1.5\%$).

4. Discussion

In the present study we assessed the structural connectivity of the anterior cingulate cortex in children with unilateral cerebral palsy as a result of periventricular white matter lesions. In particular we assessed connections to five cortical regions, selected for their high streamline count. We have examined these tracts using both the diffusion tensor model and the fibre orientation distribution, showing altered connectivity and a relationship to executive function using the Flanker task. Additionally we demonstrated a high number of crossing fibres to justify the use of a higher order model.

In addition to the ACC tracts, we analysed a previously well studied tract; the CST. Our results using the diffusion tensor model reflect previous studies (see review Scheck et al., 2012), showing reduced FA and increased MD in the hemisphere contralateral to the hemiparetic side. The AFD was also significantly reduced in this hemisphere as expected. The MD of the ipsilateral CST correlated with Flanker performance. This result is surprising as we have controlled for motor performance in the executive function task, using response time in the neutral condition as a baseline. We speculate that MD in this region is a reflection of lesion severity. MD is a measure of overall diffusion within a voxel, and therefore in our population of children with periventricular white matter lesions, increased periventricular MD likely represents a more severe lesion, which we hypothesise correlates with impaired function across multiple domains including executive function. This is consistent with the relationship not being present for either FA or AFD, suggesting that the link with executive function does not specifically relate to the CST itself. Similar findings with MD in the corona radiata and posterior limb of the internal capsule (amongst other regions) have been demonstrated previously in an ROI analysis of children with spastic diplegia, showing a correlation with both IQ and neuropsychological scores (Rai et al., 2013).

The five ACC connections studied here are all well documented anatomical connections, previously demonstrated in both primate studies and human imaging studies (Beckmann et al., 2009; Cavanna and Trimble, 2006). The changes demonstrated within these connections were overall more subtle than those in the CST. The connections between the ACC and both the rostral middle frontal gyrus and the medial orbitofrontal cortex did not show any significant differences between groups using either the diffusion tensor or FOD model. This is not surprising, as these streamlines project anteriorly from the ACC, away from the ventricles (although frontal involvement is not infrequent). The connections between the superior frontal gyrus and ACC showed significant differences between groups using diffusion tensor metrics, however, no difference using AFD. Such a result may suggest that there are changes within the region not specific to this tract, or may reflect lack of statistical power. We note that AFD was decreased in this tract bilaterally for all subjects, but not to a statistically significant level. There was a significant correlation between Flanker performance and AFD of this tract, highlighting the importance of the integrity if this tract. The superior frontal gyrus is involved in higher order cognitive tasks including spatial cognition and working memory (du Boisgueheneuc et al., 2006). Our results suggest that although this connection may not be significantly affected in children with WM lesions as a combined group, there is heterogeneous integrity of this pathway, and reduced integrity plays a role in impaired executive function. The selection criteria for this study were based on the extent of clinical impairment (GMFCS and MACS), rather than pathological extent of brain lesions; therefore frontal lobe impairment amongst these children is intrinsically heterogeneous. Those with reduced connectivity in this tract appear to have more severe executive dysfunction. Early identification of pathology in this region may therefore be able to identify children at risk of impaired executive function, where early intervention may induce plasticity (Trivedi et al., 2008; Kwon et al., 2014; Bleyenheuft et al., 2015; Englander et al., 2015).

The connection between the ACC and the precuneus showed a significant difference between groups in both AFD and MD, however, only MD was significant in post-hoc analysis. This connection is involved with higher order cognitive functions and the integration of internal and external information (Cavanna and Trimble, 2006). This also forms part of the default mode network (Buckner et al., 2008), the most highly connected network in the brain, involved with internal thought. Pathology involving this connection is likely to impact on higher order executive function, unable to be quantitatively measured with simple tasks like the Flanker task. Of all the ACC connections

examined, the connection with the precuneus runs in closest proximity to the ventricles, and is therefore more likely to be directly affected by the lesion.

The cingulum bundle itself was not significantly different between groups. This would suggest that the cingulum bundle remains relatively intact in children with white matter lesions. This is an interesting finding, as the cingulum bundle runs in close proximity to the ventricles. These results suggest that any damage to tracts connecting to the ACC occurs at a location beyond where fibres leave the cingulum bundle, with relative sparing of the cingulum bundle itself.

Our crossing fibre analysis showed that the cingulum bundle contained the fewest crossing fibres, with more than half of the voxels traversed by all tracts projecting out of the cingulate containing multiple fibre orientations. The CST showed the highest number of crossing fibres. The presence of many crossing fibres is reflected in the low mean FA values for all groups (as shown in Fig. 2). This suggests that FA group differences in these tracts are not reliable indicators of differences in connectivity. Group differences in the MD measure are more representative of underlying tissue than FA in crossing fibre regions (Jones, 2010); however MD is not tract-specific. We therefore believe that the AFD results are the most biologically interpretable and robust analysis of the tracts of interest in this study. In addition, the AFD-based connectivity measure should theoretically be more related to actual tract connectivity since it combines information from both intra-voxel fibre density and tract cross sectional area (i.e. morphological information). In contrast, the mean FA and MD for a given tract are not necessarily affected by the fibre bundle cross sectional area. For example two tracts with different cross sectional areas may have the same mean FA value, yet the thicker tract is likely to have more axons and therefore a higher 'connectivity'. The tract-specificity and additional morphological information in the AFD-derived connectivity measure is the likely cause of discrepancies between the tensor and AFD derived results (see Fig. 2). Most noticeable is the CST result (bottom row of Fig. 2). The tensor FA and MD result suggests that the CST on the hemiparetic side is spared in CP. However the AFD connectivity measure demonstrates that while the contralateral CST is most altered, the CST on the ipsilateral side also has a reduced connectivity (not statistically significant), consistent with previous studies showing reduced grey matter bilaterally in children with unilateral CP (Scheck et al., 2014). This discrepancy is likely due to a reduction in the CST width in CP, which is not detectable using FA or MD as a surrogate marker for tract connectivity. Application of this technique in children with grey matter lesions would be of particular interest, where the ipsilateral corticospinal tract undergoes hypertrophy (Eyre et al., 2007).

The AFD-based connectivity measure is, however, not without limitations. The method used in this work identifies FOD lobes belonging to the tract of interest based on streamline traversal. The entire AFD integral for a given FOD lobe is assigned to the tract providing it is associated with at least one ROI streamline. It is possible, however, that a single FOD lobe may represent axons from multiple tracts (e.g. when different tracts merge into one near the cortex). This means that the AFD-based connectivity measure for a tract of interest may not be 100% tract specific if a tract merges with another at some point along its length. While this is a limitation of the current approach, it remains a significant improvement on the diffusion tensor derived metrics, as demonstrated above. We note that a more robust method for deriving a measure of tract connectivity based on tractography and AFD would be to use Spherical deconvolution Informed Filtering of Tractograms (SIFT) (Smith et al., 2013). SIFT connectivity analysis requires robust DWI–T1 alignment to perform anatomically constrained tractography (ACT) (Smith et al., 2012) and therefore ensure that all streamlines terminate at the grey white matter interface. While we did apply field map-based EPI distortion correction to our data in this study, we found that alignment was not sufficiently accurate on our 3T-acquired data (compared with superior methods that rely on additional $b = 0$ images acquired with reverse phase encoding (Smith et al., 2012)).

The analysis approach used in this work is entirely automated, which increases reproducibility, however, it prevents the inclusion of significantly atypical brains due to the limitations of automated parcellation. This restricted our study to children with WM lesions. We attempted parcellation of 16 subjects recruited using the same protocol with cortical or deep grey matter lesions; none were able to be parcellated adequately; these children were therefore unsuitable for this study protocol. We also note that the presence of gross morphological malformations in CP prevented us from performing a whole-brain AFD fixel-based analysis (Raffelt et al., 2015) (due to imperfect image registration).

Finally, while our study had numbers comparable to other diffusion MRI studies in this population (Scheck et al., 2012), there were several trends seen which did not meet statistical significance, potentially limited by subject numbers and heterogeneity. Variation between scanning parameters and subsequent preprocessing variability presents a barrier to pooling of data across studies and centres. To increase statistical power larger trials are required, which poses a significant resource challenge.

5. Conclusion

In children with unilateral cerebral palsy due to periventricular white matter lesions, connectivity to the anterior cingulate cortex appears to be altered, playing a role in impaired executive function. Anterior projections within the frontal cortex appear to be spared, as does the cingulum bundle itself. Connectivity between the superior frontal gyrus and the anterior cingulate appears to be heterogeneously impacted, with reduced connectivity relating to impaired executive function. Early identification of damage to this tract may therefore become important when targeting early intervention. Connectivity between the anterior cingulate and the precuneus is also compromised, which may play a role in higher order cognitive difficulties. In this study we measured connectivity using diffusion tensor and FOD derived measures. The discrepancy between the results from both models is likely caused by the large number of crossing fibres in the tracts, highlighting the advantage of employing higher order models in these regions.

Appendix A. Supplementary data

Supplementary data to this article can be found online at http://dx.doi.org/10.1016/j.nicl.2015.09.014.

References

Arnfield, E., Guzzetta, A., Boyd, R., 2013. Relationship between brain structure on magnetic resonance imaging and motor outcomes in children with cerebral palsy: a systematic review. Res. Dev. Disabil. 34 (7), 2234–2250. http://dx.doi.org/10.1016/j.ridd.2013.03.031.

Bai, Y., Alexander, D.C., 2008. Model-based Registration to Correct for Motion Between Acquisitions in Diffusion MR Imaging. 5th IEEE International Symposium on Biomedical Imaging: from Nano to Macro, pp. 947–950.

Basser, P.J., Mattiello, J., LeBihan, D., 1994. MR diffusion tensor spectroscopy and imaging. Biophys. J. 66 (1), 259–267. http://dx.doi.org/10.1016/S0006-3495(94)80775-1.

Basser, P.J., Pierpaoli, C., 1996. Microstructural and physiological features of tissues elucidated by quantitative-diffusion-tensor MRI. J. Magn. Reson. B 111 (3), 209–219. http://dx.doi.org/10.1006/jmrb.1996.0086.

Beckmann, M., Johansen-Berg, H., Rushworth, M.F.S., 2009. Connectivity-based parcellation of human cingulate cortex and its relation to functional specialization. J. Neurosci. 29 (4), 1175–1190. http://dx.doi.org/10.1523/JNEUROSCI.3328-08.2009.

Bjorgaas, H.M., Hysing, M., Elgen, I., 2012. Psychiatric disorders among children with cerebral palsy at school starting age. Res. Dev. Disabil. 33 (4), 1287–1293. http://dx.doi.org/10.1016/j.ridd.2012.02.024.

Bleyenheuft, Y., Dricot, L., Gilis, N., Kuo, H.C., Grandin, C., Bleyenheuft, C., et al., 2015. Capturing neuroplastic changes after bimanual intensive rehabilitation in children with unilateral spastic cerebral palsy: a combined DTI, TMS and fMRI pilot study. Res. Dev. Disabil. 43–44, 136–149. http://dx.doi.org/10.1016/j.ridd.2015.06.014.

Bodimeade, H.L., Whittingham, K., Lloyd, O., Boyd, R.N., 2013. Executive function in children and adolescents with unilateral cerebral palsy. Dev. Med. Child Neurol. 55 (10), 926–933. http://dx.doi.org/10.1111/dmcn.12195.

Botvinick, M., Nystrom, L.E., Fissell, K., Carter, C.S., Cohen, J.D., 1999. Conflict monitoring versus selection-for-action in anterior cingulate cortex. Nature 402 (6758), 179–181. http://dx.doi.org/10.1038/46035.

Brown, J.W., 2009. Conflict effects without conflict in anterior cingulate cortex: multiple response effects and context specific representations. Neuroimage 47 (1), 334–341. http://dx.doi.org/10.1016/j.neuroimage.2009.04.034.

Buckner, R.L., Andrews-Hanna, J.R., Schacter, D.L., 2008. The brain's default network: anatomy, function, and relevance to disease. Ann. N. Y. Acad. Sci. 1–38 http://dx.doi.org/10.1196/annals.1440.011.

Bush, G., Luu, P., Posner, M.I., 2000. Cognitive and emotional influences in anterior cingulate cortex. Trends Cogn. Sci. 4 (6), 215–222. http://dx.doi.org/10.1016/S1364-6613(00)01483-2.

Caillies, S., Hody, A., Calmus, A., 2012. Theory of mind and irony comprehension in children with cerebral palsy. Res. Dev. Disabil. 33 (5), 1380–1388. http://dx.doi.org/10.1016/j.ridd.2012.03.012.

Cavanna, A.E., Trimble, M.R., 2006. The precuneus: a review of its functional anatomy and behavioural correlates. Brain 129 (3), 564–583. http://dx.doi.org/10.1093/brain/awl004.

Devinsky, O., Morrell, M.J., Vogt, B.A., 1995. Contributions of anterior cingulate cortex to behaviour. Brain 118 (1), 279–306. http://dx.doi.org/10.1093/brain/118.1.279.

Douaud, G., Jbabdi, S., Behrens, T.E.J., Menke, R.A., Gass, A., Monsch, A.U., et al., 2011. DTI measures in crossing-fibre areas: increased diffusion anisotropy reveals early white matter alteration in MCI and mild Alzheimer's disease. Neuroimage 55 (3), 880–890. http://dx.doi.org/10.1016/j.neuroimage.2010.12.008.

du Boisgueheneuc, F.d, Levy, R., Volle, E., Seassau, M., Duffau, H., Kinkingnehun, S., et al., 2006. Functions of the left superior frontal gyrus in humans: a lesion study. Brain 129 (12), 3315–3328. http://dx.doi.org/10.1093/brain/awl244.

Dunnett, C.W., 1955. A multiple comparison procedure for comparing several treatments with a control. J. Am. Statist. Assoc. 1096–1121 http://dx.doi.org/10.1080/01621459.1955.10501294.

Eliasson, A.C., Krumlinde-Sundholm, L., Rösblad, B., Beckung, E., Arner, M., Öhrvall, A.M., et al., 2006. The Manual Ability Classification System (MACS) for children with cerebral palsy: scale development and evidence of validity and reliability. Dev. Med. Child Neurol. 48 (07), 549–554. http://dx.doi.org/10.1017/S0012162206001162.

Englander, Z.A., Sun, J., Laura Case, C., Mikati, M.A., Kurtzberg, J., Song, A.W., 2015. Brain structural connectivity increases concurrent with functional improvement: evidence from diffusion tensor MRI in children with cerebral palsy during therapy. Neuroimage Clin. 7, 315–324. http://dx.doi.org/10.1016/j.nicl.2015.01.002.

Eriksen, B.A., Eriksen, C.W., 1974. Effects of noise letters upon the identification of a target letter in a nonsearch task. Perception & Psychophysics 16 (1), 143–149. http://dx.doi.org/10.3758/BF03203267.

Eyre, J.A., Smith, M., Dabydeen, L., Clowry, G.J., Petacchi, E., Battini, R., et al., 2007. Is hemiplegic cerebral palsy equivalent to amblyopia of the corticospinal system? Ann. Neurol. 62 (5), 493–503. http://dx.doi.org/10.1002/ana.21108.

Farquharson, S., Raffelt, D., Sadeghian, F., Tournier, J., Mandelstam, S., Schneider-Kolsky, M., et al., 2014. Apparent fibre density (AFD) analysis reveals decreases in axonal density in the white matter pathways of patients with grey matter heterotopia. Proceedings of the International Society for Magn Res Med, Milan, Italy.

Fischl, B., Salat, D.H., Busa, E., Albert, M., Dieterich, M., Haselgrove, C., et al., 2002. Whole brain segmentation: automated labeling of neuroanatomical structures in the human brain. Neuron 33 (3), 341–355. http://dx.doi.org/10.1016/S0896-6273(02)00569-X.

Hustad, K.C., Schueler, B., Schultz, L., Duhadway, C., 2012. Intelligibility of 4 year old children with and without cerebral palsy. J. Speech Lang. Hear. Res. 55 (4), 1177–1189. http://dx.doi.org/10.1044/1092-4388(2011/11-0083).

Iwata, S., Nakamura, T., Hizume, E., Kihara, H., Takashima, S., Matsuishi, T., et al., 2012. Qualitative brain MRI at term and cognitive outcomes at 9 years after very preterm birth. Pediatrics 129 (5), e1138–e1147. http://dx.doi.org/10.1542/peds.2011-1735.

Jenkinson, M., 2004. Improving the Registration of B0-distorted EPI Images Using Calculated Cost Function Weights. 10th International Conference on Functional Mapping of the Human Brain.

Jenkinson, M., 2003. Fast, automated, N-dimensional phase-unwrapping algorithm. Magn. Reson. Med. 49 (1), 193–197. http://dx.doi.org/10.1002/mrm.10354.

Jenkinson, M., Beckmann, C.F., Behrens, T.E.J., Woolrich, M.W., Smith, S.M., 2012. Fsl. Neuroimage 62 (2), 782–790. http://dx.doi.org/10.1016/j.neuroimage.2011.09.015.

Jeurissen, B., Leemans, A., Tournier, J.D., Jones, D.K., Sijbers, J., 2013. Investigating the prevalence of complex fiber configurations in white matter tissue with diffusion magnetic resonance imaging. Hum. Brain Mapp. 34 (11), 2747–2766. http://dx.doi.org/10.1002/hbm.22099.

Jones, D.K., 2010. Challenges and limitations of quantifying brain connectivity in vivo with diffusion MRI. Imaging Med. 2 (3), 341–355. http://dx.doi.org/10.2217/iim.10.21.

Jones, D.K., Cercignani, M., 2010. Twenty-five pitfalls in the analysis of diffusion MRI data. N.M.R. Biomed. 23 (7), 803–820. http://dx.doi.org/10.1002/nbm.1543.

Knecht, S., Drager, B., Deppe, M., Bobe, L., Lohmann, H., Floel, A., et al., 2000. Handedness and hemispheric language dominance in healthy humans. Brain 123 (12), 2512–2518. http://dx.doi.org/10.1093/brain/123.12.2512.

Krägeloh-Mann, I., Cans, C., 2009. Cerebral palsy update. Brain Dev. 31 (7), 537–544. http://dx.doi.org/10.1016/j.braindev.2009.03.009.

Krägeloh-Mann, I., Horber, V., 2007. The role of magnetic resonance imaging in elucidating the pathogenesis of cerebral palsy: a systematic review. Dev. Med. Child Neurol. 49 (2), 144–151. http://dx.doi.org/10.1111/j.1469-8749.2007.00144.x.

Kwon, J., Chang, W.H., Chang, H.J., Yi, S., Kim, M., Kim, E., et al., 2014. Changes in diffusion tensor tractographic findings associated with constraint-induced movement therapy in young children with cerebral palsy. Clin. Neurophys. 125 (12), 2397–2403. http://dx.doi.org/10.1016/j.clinph.2014.02.025.

Mori, S., Crain, B.J., Chacko, V.P., van Zijl, P.C.M., 1999. Three-dimensional tracking of axonal projections in the brain by magnetic resonance imaging. Ann. Neurol. 45 (2), 265–269. http://dx.doi.org/10.1002/1531-8249(199902)45:2<265::AID-ANA21>3.0.CO;2-3.

Morris, D., Nossin-Manor, R., Taylor, M.J., Sled, J.G., 2011. Preterm neonatal diffusion processing using detection and replacement of outliers prior to resampling. Magn. Reson. Med. 66 (1), 92–101. http://dx.doi.org/10.1002/mrm.22786.

Nam, H., Park, H.J., 2011. Distortion correction of high b-valued and high angular resolution diffusion images using iterative simulated images. Neuroimage 57 (3), 968–978. http://dx.doi.org/10.1016/j.neuroimage.2011.05.018.

Novak, I., Hines, M., Goldsmith, S., Barclay, R., 2012. Clinical prognostic messages from a systematic review on cerebral palsy. Pediatrics 130 (5), e1285-312. http://dx.doi.org/10.1542/peds.2012-0924.

Pannek, K., Boyd, R.N., Fiori, S., Guzzetta, A., Rose, S.E., 2014. Assessment of the structural brain network reveals altered connectivity in children with unilateral cerebral palsy due to periventricular white matter lesions. Neuroimage Clin. 5, 84–92. http://dx.doi.org/10.1016/j.nicl.2014.05.018.

Pannek, K., Mathias, J.L., Bigler, E.D., Brown, G., Taylor, J.D., Rose, S., 2010. An automated strategy for the delineation and parcellation of commissural pathways suitable for clinical populations utilising high angular resolution diffusion imaging tractography. Neuroimage 50 (3), 1044–1053. http://dx.doi.org/10.1016/j.neuroimage.2010.01.020.

Pannek, K., Raffelt, D., Bell, C., Mathias, J.L., Rose, S.E., 2012. HOMOR: higher order model outlier rejection for high b-value MR diffusion data. Neuroimage 63 (2), 835–842. http://dx.doi.org/10.1016/j.neuroimage.2012.07.022.

Paus, T., 2001. Primate anterior cingulate cortex: where motor control, drive and cognition interface. Nat. Rev. Neurosci. 2 (6), 417–424. http://dx.doi.org/10.1038/35077500.

Pierpaoli, C., Barnett, A., Pajevic, S., Chen, R., Penix, L., Virta, A., et al., 2001. Water diffusion changes in Wallerian degeneration and their dependence on white matter architecture. Neuroimage 13 (6), 1174–1185. http://dx.doi.org/10.1006/nimg.2001.0765.

Raffelt, D., Cheong, J., Sadeghian, F., Thompson, D., Anderson, P., Doyle, L., et al., 2014a. Apparent fibre density abnormalities in adolescents born extremely preterm: moving beyond the diffusion tensor. Proceedings of the International Society for Magn Res Med, Milan, Italy.

Raffelt, D., Parker, D., McMahon, J., Scheffer, I., Connelly, A., 2014b. Decreased apparent fibre density in Dravet syndrome. Proceedings of the International Society for Magn Res Med, Milan, Italy.

Raffelt, D., Smith, R., Tournier, J., Ridgway, G., Villemagne, V., Rowe, C., et al., 2013. Tractographic threshold-free cluster enhancement: whole-brain statistical analysis of diffusion MRI measures in the presence of crossing fibres. Proceedings of the International Society for Magn Res Med, Salt Lake City, UT, USA.

Raffelt, D., Tournier, J., Crozier, S., Ellis, K., Martins, R., Villmagne, V.L., et al., 2012b. Voxel-based analysis of Alzheimer's Disease using apparent fibre density. International Society for Magn Res Med 20th Annual Meeting.

Raffelt, D., Tournier, J.-D., Rose, S., Ridgway, G.R., Henderson, R., Crozier, S., et al., 2012a. Apparent fibre density: a novel measure for the analysis of diffusion-weighted magnetic resonance images. Neuroimage 59 (4), 3976–3994. http://dx.doi.org/10.1016/j.neuroimage.2011.10.045.

Raffelt, D.A., Smith, R.E., Ridgway, G.R., Tournier, J., Vaughan, D.N., Rose, S., et al., 2015. Connectivity-based fixel enhancement: whole-brain statistical analysis of diffusion MRI measures in the presence of crossing fibres. Neuroimage 117, 40–55. http://dx.doi.org/10.1016/j.neuroimage.2015.05.039.

Rai, Y., Chaturvedi, S., Paliwal, V.K., Goyal, P., Chourasia, A., Singh Rathore, R.K., et al., 2013. DTI correlates of cognition in term children with spastic diplegic cerebral palsy. Eur. J. Paediatr. Neurol. 17 (3), 294–301. http://dx.doi.org/10.1016/j.ejpn.2012.11.005.

Russell, D.J., Rosenbaum, P.L., Cadman, D.T., Gowland, C., Hardy, S., Jarvis, S., 1989. The gross motor function measure: a means to evaluate the effects of physical therapy. Dev. Med. Child Neurol. 31 (3), 341–352. http://dx.doi.org/10.1111/j.1469-8749.1989.tb04003.x.

Scheck, S.M., Boyd, R.N., Rose, S.E., 2012. New insights into the pathology of white matter tracts in cerebral palsy from diffusion magnetic resonance imaging: a systematic review. Dev. Med. Child Neurol. 54 (8), 684–696. http://dx.doi.org/10.1111/j.1469-8749.2012.04332.x.

Scheck, S.M., Pannek, K., Fiori, S., Boyd, R.N., Rose, S.E., 2014. Quantitative comparison of cortical and deep grey matter in pathological subtypes of unilateral cerebral palsy. Dev. Med. Child Neurol. 56 (10), 968–975. http://dx.doi.org/10.1111/dmcn.12461.

Smith, R.E., Tournier, J.D., Calamante, F., Connelly, A., 2012. Anatomically-constrained tractography: improved diffusion MRI streamlines tractography through effective use of anatomical information. Neuroimage 62 (3), 1924–1938. http://dx.doi.org/10.1016/j.neuroimage.2012.06.005.

Smith, R.E., Tournier, J.D., Calamante, F., Connelly, A., 2013. SIFT: spherical-deconvolution informed filtering of tractograms. Neuroimage 67, 298–312. http://dx.doi.org/10.1016/j.neuroimage.2012.11.049.

Stejskal, E.O., 1965. Use of spin echoes in a pulsed magnetic-field gradient to study anisotropic, restricted diffusion and flow. J. Chem. Phys. 43 (10), 3597. http://dx.doi.org/10.1063/1.1696526.

Tournier, J., Calamante, F., Connelly, A., 2007. Robust determination of the fibre orientation distribution in diffusion MRI: non-negativity constrained super-resolved spherical deconvolution. Neuroimage 35 (4), 1459–1472. http://dx.doi.org/10.1016/j.neuroimage.2007.02.016.

Tournier, J., Counsell, S., Raffelt, D., Tusor, N., Nongena, P., Edwards, D., et al., 2013. High b-value HARDI analysis in neonates scanned at term-equivalent age reveals correlation between apparent white matter fibre density and immaturity at birth. Proceedings of the International Society for Magn Res Med, Salt Lake City, UT, USA.

Tournier, J.-D., Calamante, F., Gadian, D.G., Connelly, A., 2004. Direct estimation of the fiber orientation density function from diffusion-weighted MRI data using spherical deconvolution. Neuroimage 23 (3), 1176–1185. http://dx.doi.org/10.1016/j.neuroimage.2004.07.037.

Trivedi, R., Gupta, R.K., Shah, V., Tripathi, M., Rathore, R.K.S., Kumar, M., et al., 2008. Treatment-induced plasticity in cerebral palsy: a diffusion tensor imaging study. Pediatr. Neurol. 39 (5), 341–349. http://dx.doi.org/10.1016/j.pediatrneurol.2008.07.012.

Vaughan, D., Raffelt, D., Tournier, J., Jackson, G., Connelly, A., 2013. Apparent fibre density shows tract-specific white matter changes in temporal lobe epilepsy. Proceedings of the International Society for Magn Res Med, Salt Lake City, UT, USA.

Weierink, L., Vermeulen, R.J., Boyd, R.N., 2013. Brain structure and executive functions in children with cerebral palsy: a systematic review. Res. Dev. Disabil. 34 (5), 1678–1688. http://dx.doi.org/10.1016/j.ridd.2013.01.035.

Whittingham, K., Bodimeade, H.L., Lloyd, O., Boyd, R.N., 2014. Everyday psychological functioning in children with unilateral cerebral palsy: does executive functioning play a role? Dev. Med. Child Neurol. 56 (6), 572–579. http://dx.doi.org/10.1111/dmcn.12374.